

Analysis of Convolutional Neural Network for Fundus Image Segmentation

A S Shirokanev^{1,2,a}, N Yu Ilyasova^{1,2,b} and N S Demin^{1,2,c}

¹IPSI RAS - branch of the FSRC «Crystallography and Photonics» RAS, Molodogvardejskaya street 151, Samara, Russia, 443001

²Samara National Research University, Moskovskoe Shosse 34A, Samara, Russia, 443086

Emails:^a alexandrshirokanev@gmail.com; ^bilyasova.nata@gmail.com;
^cnikitos361@yandex.ru

Abstract. In this paper the study of fundus image segmentation using convolutional neural networks is carried out. A neural network architecture was made to classify four classes of images, which are made up of thick and thin blood vessels, healthy areas, and exudate areas. The CNN architecture was constructed empirically so as the required accuracy of no less than 96 % is ensured. The segmentation error was calculated on the exudates class, which is key for laser coagulation surgery. In the paper we utilized the HSL color model because it renders color characteristics of eye blood vessels and exudates most adequately. We have demonstrated the H channel to be most informative. We have investigated the robustness of technology to various noises. Experimental studies have shown the instability of the convolutional neural network to Gaussian white noise and resistance to impulse noise.

1. Introduction

Diabetes mellitus is one of the most common and dangerous endocrine diseases in the world. Due to changes in the blood vessels of the retina in diabetes, a dangerous complication called diabetic retinopathy (DR) can develop. In DR, all parts of the retina are affected, but due to changes in the central regions in the form of diabetic macular edema, a rapid and irreversible decrease in vision occurs [1-3]. According to the research, accurate and early diagnosis, as well as timely and correct treatment can prevent total blindness in more than 50% of cases [4,5]. At the moment there are several ways to treat. Medication with the use of anti-VEGF drugs [6-8], as well as laser coagulation, the effectiveness of which was confirmed during a large study (ETDRS, 1987) and today is the “gold standard” for the treatment of DR [8].

In the course of laser therapy, a series of dosed microscopic thermal wounds (laser coagulates) are inflicted in the macular edema area. Conducted various research to reduce the traumatic effect of this operation, as well as to increase the accuracy and speed of this procedure. Currently, laser systems with the possibility of automatically applying coagulates using preselected patterns are widely used [9] (Figure 1). However, this technique does not always allow to achieve the desired therapeutic effect. In this regard, researches were conducted on the development of algorithms for the optimal filling of edema with coagulates. The research results are presented in [10, 11]. The arrangement of coagulates by the proposed algorithms is carried out in a selected area of edema, which is formed based on the



result of segmentation of the fundus image. The researchers have come up with a number of solutions based on feature generation via discriminative analysis [12].

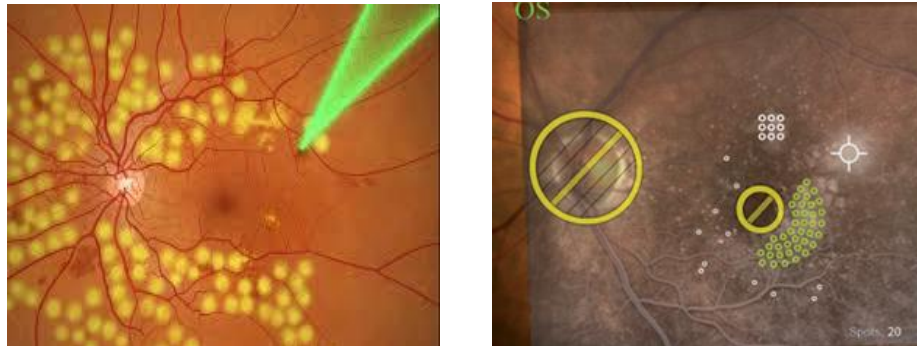


Figure 1. Examples of laser coagulation of retina and pattern examples of the software NAVILAS [9].

Convolutional neural networks are more preference when using for object classification [13] according to the conclusion members of the research community. May 2006 has seen the publication of the first issue of IEEE Transaction on. The first detailed review of the use of deep learning for medical image analysis published in 2017 [14]. Today an active trend for the development of digital medicine is seen. For example a classification model based on a convolutional neural network was used for diagnosing the H. Pylori infection [15]. In the work, architecture specially oriented to solve a particular problem. The authors came to the conclusion that the particular disease was possible to diagnose based on endoscopic images obtained using CNN. In Ref. [16], diagnosing an early-stage hypertension retinopathy was discussed. One of the causes of eye diseases is blood hypertension. The classifier proposed in Ref. [16] offered a 98.6 percent accuracy. In Ref. [17], a toolkit was developed for the automated analysis of psoriasis-affected skin biopsy images, which is of considerable significance in clinical treatment. The paper is a pioneering attempt into automatic segmentation of psoriasis-affected skin biopsy images. The study resulted in a practical system based on the machine analysis. CNN training on a prepared dataset was demonstrated, intended for further analysis of input images. In this work, we study a class of eye fundus images with pathological changes that can be found at different stages of the disease. The diabetic retinopathy results in appearing of exudates, which cause the retina thickening. Usually, the fundus image contains four classes of objects, such as thick and thin blood vessels, healthy areas and exudate zones.

2. Training the convolutional neural network

The initial data for analysis contained 11 training datasets of various size. All datasets were balanced and in total contained 534 images. For the purposes of the present work, the CNN training was conducted on four above-described classes of eye fundus images. The initial dataset consisted of 75 percent of training images and 25 percent of test images. To prevent overtraining, a control dataset was also used. A 3x3 convolution kernel was chosen because it is optimal for 12x12 images. The CNN architecture was constructed empirically so as the required accuracy of no less than 96 % is ensured. Table 1 gives architecture of the empirically constructed convolutional neural network. With this architecture, a recognition accuracy of 99.3% was attained, which is the best recognition result for the four above-mentioned classes of images. Figure 2 shows a dependency of learning error on the number of epochs. To attain a recognition certainty of 95 %, the CNN was put through 120 training runs on the initial images of all sizes. Figure 3 shows an average training result for each image size. The results in Figure 2 show that the highest classification accuracy is attained for 12x12 images.

3. Experimental study

For the experiments, datasets were formed containing four above-described classes of 12x12 images, using which the best result of CNN testing is achieved (Figure 3). In this study, the segmentation of

eye fundus images was conducted via deep learning. Shown in Figure 4a is the result of CNN-aided image segmentation. With a view of estimating the CNN-aided segmentation error, a manual segmentation by an expert ophthalmologist was introduced as a reference image (Figure 4b). The study was conducted on the exudates class, which had been singled out into a separate image (Figure 4c). The error of CNN-aided segmentation of the said exudate areas was calculated relative to the expert estimate. The result of comparison of the exudation areas highlighted by CNN (Figure 4d) and the expert (Figure 4c) is shown in Table 2.

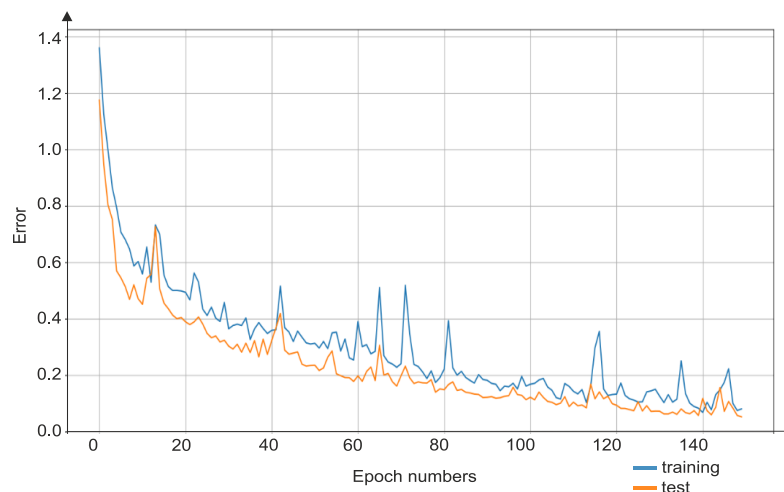


Figure 2. The dependency of learning error on the number of epochs.

Table 1. Architecture of the convolutional neural network.

Layer number	Layers	Parameters	Layer number	Layers	Parameters
1	Convolutional	300 neurons	3	Activation	Function: RELU
1	Activation	Function: RELU	4	Convolutional	150 neurons
2	Convolutional	300 neurons	4	Activation	Function: RELU
2	Activation	Function: RELU	4	MaxPooling	Size: 2×2
2	Dropout	0.5	4	Dropout	0.5
2	MaxPooling	Size: 2×2	5	Fully-connected	4
3	Convolutional	150 neurons	5	Activation	softmax

Using the data from Table 2, a CNN-aided segmentation error for the exudates was defined as $E = (k + t) / NM$ and amounted to 7% (where $N \times M$ is the image size, k is the number of expert-highlighted pixels that CNN failed to recognize as exudates, t is the number of exudate pixels recognized by CNN but missing from the expert's image). The error of first kind, defined as $E_1 = l / F$, where l is the number of falsely recognized exudates classes and F is the total number of exudate-containing pixels in the expert's image, amounted to 5%.

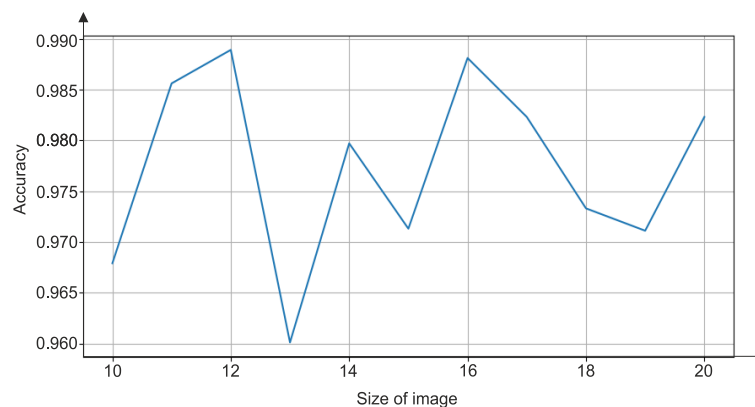


Figure 3. The dependence of accuracy on the size of images in the training set.

In the process of exudates area identification, color plays a key role. The segmentation error can be significantly reduced by operating in particular color spaces. It has been established [18] that color models YUV, RGB and HSL are most close to color perception of the human eye. However, the models RGB and YUV have a number of hardware limitations with certain video-systems. In further research, we used the HSL color model as the one that most adequately renders the color characteristics of blood vessels and exudates. Figure 4b shows pathological areas highlighted by the expert in different HSL color channels. Veracity of CNN-aided exudate highlighting has been confirmed by comparison of histograms of CNN-aided and expert's images (Figure 5), which were superimposed for each corresponding channel of HSL color system, with the expert-based histograms marked as green bars, and the CNN-based histograms marked red (Figure 5).

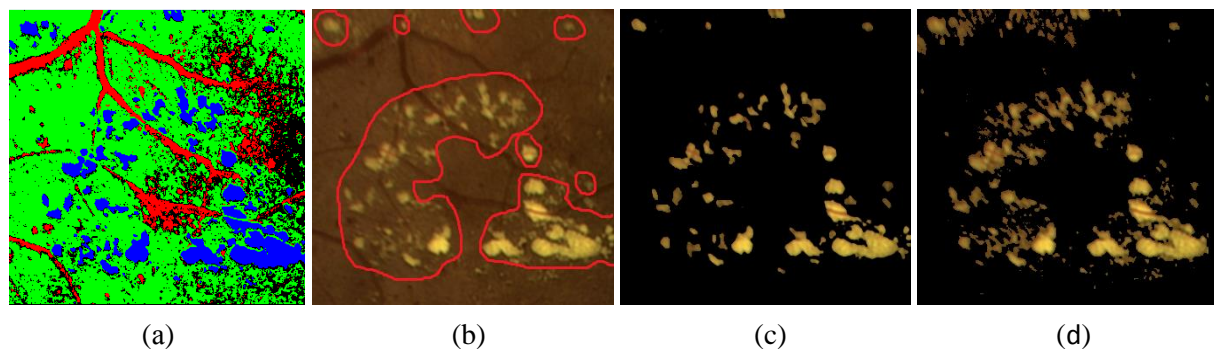


Figure 4. Four classes of objects highlighted in the image using CNN (a); exudates areas manually outlined by an expert (b); exudates class highlighted by an expert (c) and using the CNN technique (d).

Table 2. Percentage of exudates areas in the image.

Areas	Percentage of exudates area, %
Exudates area in the expert's image	9
Exudates area in the CNN-aided image	15
Total exudates area	95.6
Expert's exudates areas omitted by CNN	0.4
CNN-highlighted exudates areas missing in the expert's image	6

The expert-based histograms define an interval of values for the affected fundus areas (Figure 6).

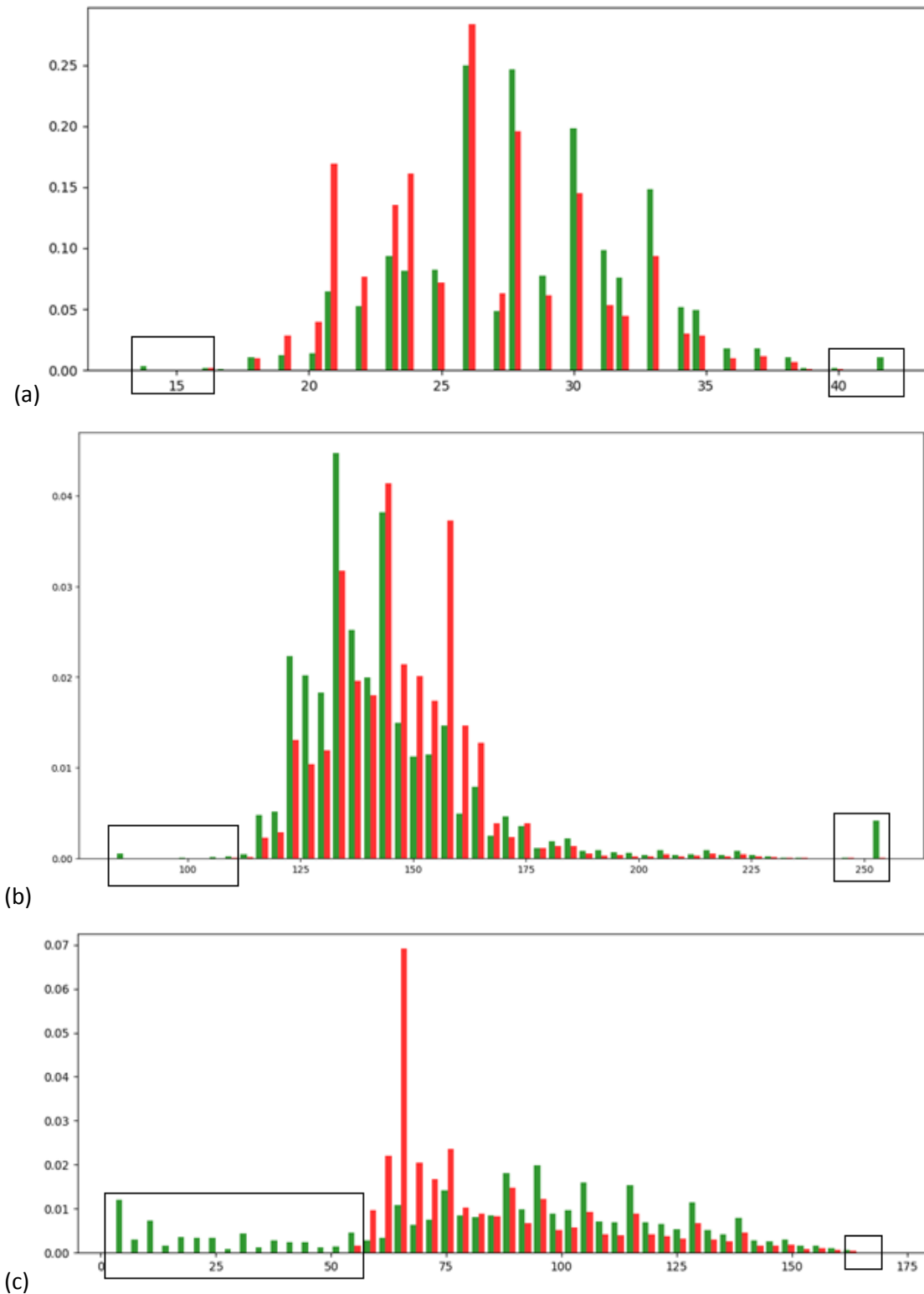


Figure 5. Histograms obtained by using an expert opinion and CNN: (a) H, (b) S, and (c) L channels.

From the histograms, the CNN-aided interval of exudates area is seen to be narrower than that obtained based on expert's estimates. The histogram regions corresponding to the false CNN-aided classification are within intervals shown by rectangles (Figure 5). Table 3 gives segmentation errors

calculated for each channel of the HSL color model. The data in Table 3 suggest that the H channel is the most informative channel with the least segmentation error.

4. Investigation of the segmentation robustness to various noises based on the convolutional neural network

In this paper, we investigated the robustness of technology to various noises. A study was conducted of the stability of the neural network to blur, Gaussian noise and impulse noise. For the fundus image blurred by averaging 5×5 mask the neural network provides a robustness segmentation result when blurring. Figure 6 shows the image to which white noise with a variance of 0.01 was added, and the image obtained as a result of segmentation. The neural network exhibits unstable segmentation in various images distorted by Gaussian noise. An example of unstable segmentation is shown in Figure 6b. The original image was also subjected to distortion by impulse noise. Figure 6c shows image distorted by impulse noise with a density of 0.05. The neural network to this noise is most robustness. Impulse noise may appear on the image due to the technical features of the fundus camera, as a result of which impulse noise robustness is important. The study showed that the most informative channel is channel H.

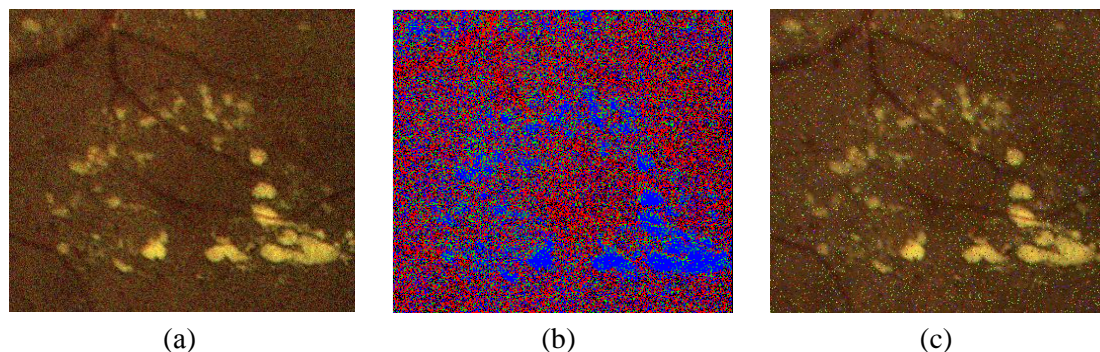


Figure 6. Source fundus image and segmentation result: a) gaussian white noise with a dispersion of 0.01, b) CNN result, c) impulse noise with a density of 0.05.

Table 3. Segmentation error in impulse noise image.

Dispersion	Error of the first kind, %
0.05	43
0.10	62
0.50	86

The error of the first kind was calculated for this channel. Table 3 shows the dependence of the error on the pixel density of the pulsed noise. The convolution network has the highest robustness to impulse noise than to other noises, which is important when taking into account the technical features of the camera.

5. Conclusion

In this work, a convolutional neural network (CNN) has been applied to the analysis of an eye fundus image. CNN architecture has been constructed, allowing a testing error of no more than 4% to be attained. Based on a 3×3 convolution kernel, CNN training was conducted on 12×12 images, thus enabling the best result of CNN testing to be achieved. CNN-aided segmentation of the input image conducted in this work has shown the CNN to be capable of identifying all training dataset classes with high accuracy. The segmentation error was calculated on the exudates class, which is key for laser coagulation surgery. The segmentation error on the exudates class was 7 %, with the error of first kind being 5 %. In the study, we utilized the HSL color model because it renders color characteristics of eye blood vessels and exudates most adequately. We have demonstrated the H channel to be most informative, with the segmentation error amounting to 3 %. We investigated the robustness of

technology to various noises. Experimental studies have shown the instability of the convolutional neural network to Gaussian white noise and resistance to impulse noise.

Acknowledgements

This work was financially supported by the Russian Foundation for Basic Research under grant # 19-29-01135, # 17-01-00972 and by the Ministry of Science and Higher Education within the State assignment to the FSRC “Crystallography and Photonics”.

References

- [1] Doga A. V., Kachalina G. F., Pedanova E. K. and Buryakov D. A. 2014. Modern diagnostic and treatment aspects of diabetic macular edema. *Ophthalmology, Diabetes*. **4** 51-59
- [2] Whiting D.R. 2011. IDF diabetes atlas: global estimates of the prevalence of diabetes for 2011 and 2030. *Diabetes Res. Clin. Pract.* **94**(3) 311-321
- [3] Bratko G.V., Chernykh V.V., Sazonova O.V. 2015. On the issue of early diagnosis and the frequency of occurrence of diabetic macular edema and the formation of risk groups for its development. *Siberian Journal of Medical Scientific Research*. **35**(1) 33-36
- [4] Zamytskiy E. A. 2017. Analysis of the coagulates intensity in laser treatment of diabetic macular edema in a Navilas robotic laser system. *Saratov Journal of Medical Scientific Research*. **13**(2) 375-378
- [5] Amirov A.N., Abdulaeva E.A., Minkhuzina E.L. 2015. Diabetic macular edema: epidemiology, pathogenesis, diagnosis, clinical presentation, treatment. *Kazan Medical Journal*. **96**(1) 70-74
- [6] Iskhakova A.G. 2014. The results of clinical and economic analysis of the treatment of patients with diabetic retinopathy with macular edema. *Post-graduate herald of the Volga region*. **1** 96-98
- [7] Umanets N.N., Rozanov Z.A., Maher A. 2013. Intravitreal injection of ranibizumab as a method of treating patients with cystic diabetic macular edema. *Ophthalmologic journal*. **2** 56-60
- [8] Astakhov Y. S., Shadrichiev F. E., Krasavina M. I. and Grigoryeva N. N. 2009. Modern approaches to the treatment of a diabetic macular edema. *Ophthalmologic sheets*. **4** 59-69
- [9] Kernt M., Cheuteu R. and Liegl R. 2012. Navigated focal retinal laser therapy using the NAVILAS® sys-tem for diabetic macula edema. *Ophthalmologe*. **109** 692-700
- [10] Ilyasova N., Kirsh D., Paringer R., Kupriyanov A. and Shirokanev A. 2017. Coagulate map formation algorithms for laser eye treatment. *IEEE Xplore*. 1-5
- [11] Shirokanev A. S., Kirsh D. V., Ilyasova N. Yu. and Kupriyanov A. V. 2018. Investigation of algorithms for coagulate arrangement in fundus images. *Computer Optics*. **42**(4) 712-721
- [12] Ilyasova N. Yu., Kupriyanov A. V. and Paringer R. A. 2014. Formation of features for improving the quality of medical diagnosis based on discriminant analysis methods. *Computer Optics*. **38**(4) 851-855
- [13] Guido S, Andreas C 2017 Introduction to machine learning with python. *O'Reilly Media* 392
- [14] Litjens G A 2017 survey on deep learning in medical image analysis. *Medical Image Analysis* **42** 60-88
- [15] Shichijo S et al 2017 Application of Convolutional Neural Networks in the Diagnosis of Helicobacter pylori Infection Based on Endoscopic Images. *The LANCET* **25** 106-111
- [16] Bambang K T 2017 The Classification of Hypertensive Retinopathy using Convolutional Neural Network. *ICCSCI* 166-173
- [17] Anabik P 2018 Psoriasis skin biopsy image segmentation using Deep Convolutional Neural Network. (*Computer Methods and Programs in Biomedicine* vol 159) pp 59-69
- [18] Nikitaev V G 2004 Experimental study of color models in automated image analysis tasks (*Scientific session MIFI* vol 1) pp 253-25